High-Frequency Impedance of Semiconductor Superlattice Elements in External Resonance System

V. V. Makarov[a, b]*, V. A. Maksimenko[a, b],
A. A. Koronovskii[a, b], Yu. M. Skvortsova[a], and A. E. Hramov[a, b]

[a] Yury Gagarin State Technical University of Saratov, Saratov, 410054 Russia
[b] Saratov State University, Saratov, 410012 Russia
*e-mail: vladmak404@gmail.com

Received December 23, 2014

Abstract—We have studied the high-frequency (HF) impedance of a semiconductor superlattice coupled to an external electrodynamic system, which is a promising element of devices for terahertz (THz) and sub-THz frequency ranges. A characteristic behavior of the impedance under the action of an external harmonic HF signal in the region of synchronization at the fundamental and high-order resonance frequencies of the domain transport system is determined. It is shown that the diagnostics of synchronous regimes in a semiconductor superlattice in an external resonator can be based on analysis of the dynamics of amplitude and phase of the HF impedance.

At present, one of the most important tasks related to exploration of the terahertz (THz) and sub-THz frequency ranges is the creation of semiconductor devices capable of operating in a broad temperature range, which is necessary for their practical application. A promising element of these devices for the THz range is a semiconductor superlattice (SL) representing alternating micron-thick layers of two or more semiconducting materials with various bandgap widths [1–3]. This periodic structure is capable of forming energy minibands, in which electrons exhibit interesting quantum effects such as the Wannier–Stark ladder, seral and resonant tunneling, and Bloch oscillations [4, 5]. In addition, the free motion of electrons in these minibands favors the development of instabilities upon when a certain critical magnitude of the applied electric field is exceeded, this leading to the formation of domains with a strong charge concentration. The frequency of passage of these domains through a nanostructure can reach several dozen or hundreds of gigahertz [6]. An important feature of semiconductor SLs is their ability to operate at room temperature [7], which makes these elements promising sources of sub-THz and THz oscillations [7–10].

It was previously demonstrated [10] that studying the dynamics of semiconductor SLs in external resonance systems is a topical task because active semiconductor elements in real devices are always integrated into external electrodynamic structures. It has been found that a resonance system favors the formation of broad regions of chaotic dynamics in the system and makes it possible to effectively control the power and frequency spectrum of electromagnetic radiation generated by the semiconductor SL. In this context, it is important to study the high-frequency (HF) impedance of a semiconductor SL [11] coupled to a resonance system, which will allow a detailed analysis of the behavior of this system in various electronic schemes with SLs acting as generators or amplifiers of signals in the sub-THz and THz ranges.

In the present work, we have studied the HF impedance of a semiconductor SL coupled to an external electrodynamic system and determined the characteristic behavior of the impedance under the action of an external harmonic HF signal in the region of synchronization at the fundamental and high-order resonance frequencies of the domain transport system.

The collective dynamics of charge in a semiconductor SL is described here using a standard model presented in detail elsewhere [7–9, 12], which is based on a self-consistent system of the Poisson's and continuity equations. The system has been numerically integrated with physical parameters of the SL selected for an experimental prototype studied in [10]. Note that the SL properties in this work were determined at low temperatures, where the diffusion component of current density could be ignored.

The external resonance circuit is modeled in a single-mode approximation, in which a resonator with an
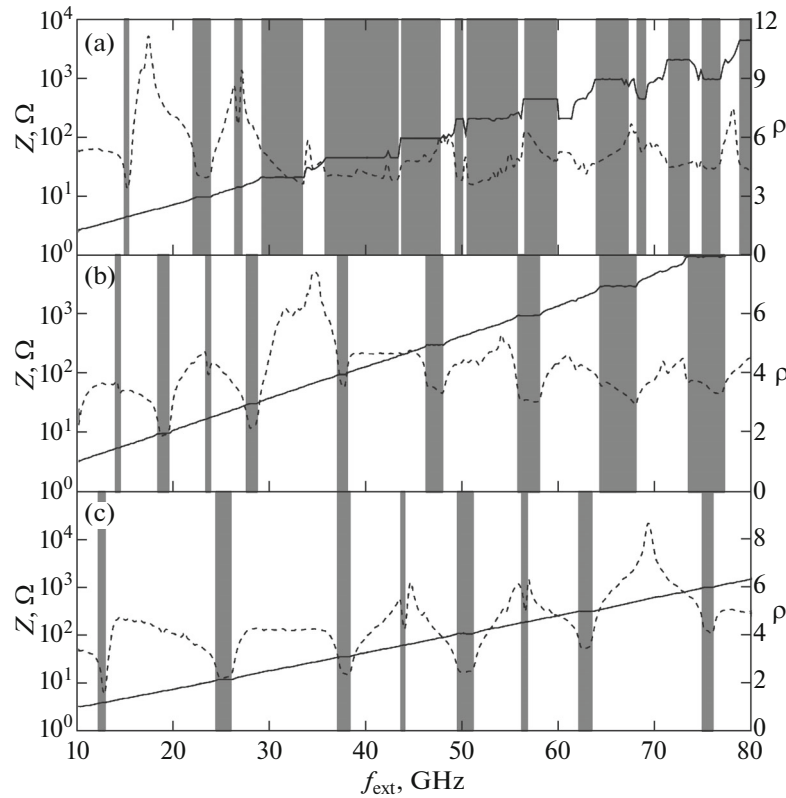
Fig. 1. Impedance amplitude Z (dashed line) and rotational index ρ (solid line) as functions of the external signal frequency f_{ext} for various harmonics of the external resonator (GHz): (a) 17.3, (b) 34.6, and (c) 69.2. Calculations for $Q = 750$, bias voltage $V_0 = 510$ mV, and external signal amplitude $V_m = 20$ mV.

equivalent scheme [10] is described by the following Kirchhoff equations:

$$C\frac{dV_1}{dt} = I(V_{sl}) - I_1, \qquad (1)$$

$$L\frac{dI_1}{dt} = V_{sl} - V - R_1 I_1 + I(V_{sl})R_1, \qquad (2)$$

where $I(V_{sl})$ is the current generated by the SL. The resonator is characterized by frequency f_Q and figure of merit Q. Voltage $V(t)$ applied to the SL is expressed as $V(t) = V_0 + V_{ext}$, where V_0 is the constant component and V_{ext} is the alternating external signal

$$V_{ext} = V_m \cos(2\pi f_e t). \qquad (3)$$

In order to calculate the impedance, the waveform of SL current oscillations was expanded into the Fourier spectrum in which a harmonic corresponding to the frequency (f_e) of external signal was found. Amplitude $|Z|$ and phase φ_z of the impedance were calculated as [13]

$$|Z| = V_m/I(f_e), \qquad \varphi_Z = \varphi_U - \varphi_I(f_e),$$

where $I(f_e)$ is the amplitude of the current harmonic with the external signal frequency, $\varphi_I(f_e)$ is the phase of this harmonic determined from the Fourier spectrum,

and φ_U is the phase of the external signal. The diagnostics of synchronization in the system was based on "rotational index" ρ defined as the ratio of the external signal frequency to the fundamental frequency of oscillations in the system.

Figures 1 and 2 show dependences of the HF impedance on the frequency of the external signal calculated using the above model for a fixed amplitude of this signal $V_m = 20$ mV and various frequencies of the external resonator. Gray bands indicate the regions of synchronization, which corresponds to rational values $\rho = f_e/f_0$ of the rotational index, where f_0 is the frequency of oscillations of the current passing in the SL. The frequencies of the external resonator were selected based on the fundamental frequency of the domain transport in the autonomous SL (which is 17.3 GHz at an applied voltage of 510 mV) and corresponded to the first, second, and fourth harmonics (Figs. 1a–1c, respectively). For the sake of convenience, all frequency dependences of Z are plotted on a logarithmic scale.

As can be seen from Figs. 1a and 1c, the impedance amplitude is maximum at the resonator frequency and increases in asynchronous regimes. The appearance of synchronization is accompanied by a sharp drop in the impedance, while the breakage of the synchronous
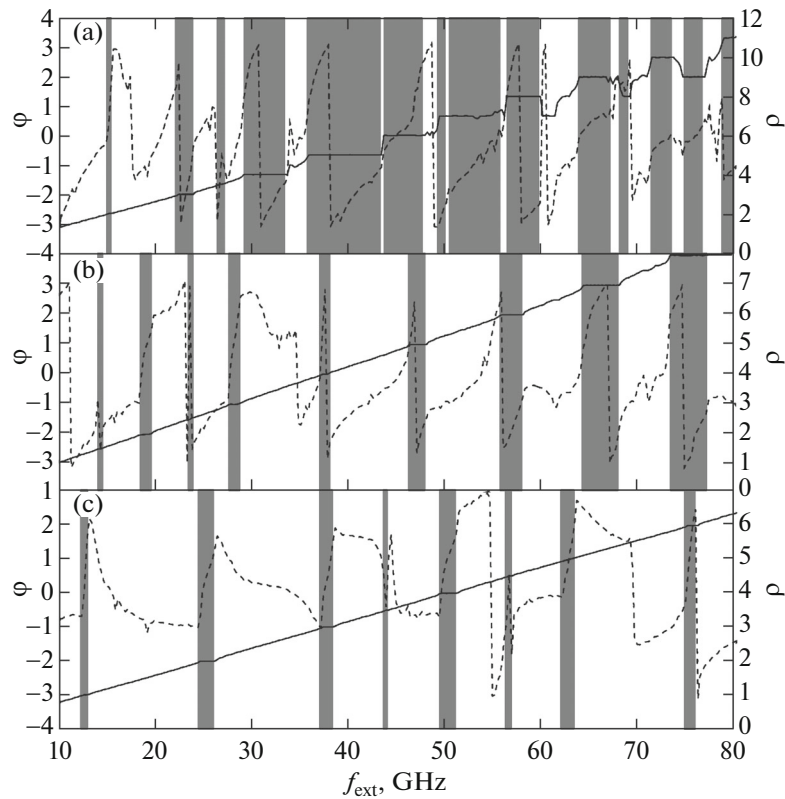
Fig. 2. Impedance phase φ (dashed line) and rotational index ρ (solid line) as functions of the external signal frequency f_{ext} for various harmonics of the external resonator (GHz): (a) 17.3; (b) 34.6; (c) 69.2. Calculations for $Q = 750$, bias voltage $V_0 = 510$ mV, and external signal amplitude $V_m = 20$ mV.

state leads to its increase. This tendency is less pronounced at higher harmonics and small detunings between the resonator frequency and eigenfrequencies of SL oscillations (Fig. 1a), which is related to realization of the regimes of irregular dynamics and transitions between chaotic and periodic regimes with variable parameters [10, 14, 15]. The observed effect is of interest for experimental investigations of SLs as HF signal amplifiers, since it can be used for detecting synchronous regimes from a change in the system impedance measured with the aid of network analyzers. It should be noted that jumps of the impedance amplitude at boundaries of the synchronous state become more pronounced with increasing frequency of the resonator, which gives grounds to believe that the proposed method of synchronization diagnostics is applicable in the sub-THz and THz range where direct measurements are difficult.

Consider the dynamics of the impedance phase plotted versus external signal frequency in Figs. 2a–2c. As can be readily seen, the phase is also highly sensitive to establishment of synchronous regimes in the system. The impedance phase slowly increases with the frequency of the external signal in asynchronous regimes and sharply grows in a synchronous state. In

addition, the phase exhibits a sharp jump at the resonance frequency of the external resonator, which can be used for monitoring of the characteristics of parasitic resonance circuits formed by contacts of a nanostructure.

In conclusion, the present work was devoted to studying the HF impedance of a semiconductor SL coupled to an external electrodynamic resonance system, which is a promising element of devices for sub-THz and THz frequency ranges. The behavior of the impedance at various frequencies of the external resonator has been studied, and its characteristic features at the boundary of synchronous states and outside the regions of synchronism have been determined. The observed effects are of importance for diagnostics of synchronous regimes in experimental investigations and for the creation of HF signal amplifiers based on semiconductor SLs.

REFERENCES

1. M. I. Ovsyannikov, Yu. A. Romanov, V. N. Shabanov, and R. G. Loginova, Sov. Phys. Semicond. **4** (12), 1919 (1970).

2. A. Ya. Shik, Sov. Phys. Semicond. **8** (10), 1195 (1974).

3. L. Esaki and R. Tsu, IBM J. Res. Dev. **14** (1), 61 (1970).

4. L. L. Bonilla and H. T. Grahn, Rep. Prog. Phys. E **68** (3), 577 (2005).

5. K. Hofbeck, J. Grenzer, E. Schomburg, et al., Phys. Lett. A **218**, 349 (1996).

6. H. Eisele et al., Appl. Phys. Lett. **96**, 072101 (2010).

7. A. O. Selskii, A. A. Koronovskii, A. E. Hramov, et al., Phys. Rev. B **84**, 235311 (2011).

8. R. Tsu, *Superlattices to Nanoelectronics* (Elsevier Science, Amsterdam, 2005).

9. A. Wacker, Phys. Rep. **357** (1), 121 (2002).

10. A. E. Hramov, V. V. Makarov, A. A. Koronovskii, et al., Phys. Rev. Lett. **112**, 116603 (2014).

11. V. V. Makarov, O. I. Moskalenko, A. A. Koronovskii, A. E. Hramov, and A. G. Balanov, Bull. Russ. Acad. Sci.: Phys. **76** (12), 1316 (2012).

12. A. G. Balanov, M. T. Greenaway, A. A. Koronovskii, O. I. Moskalenko, A. O. Sel'skii, T. M. Fromhold, and A. E. Hramov, J. Exp. Theor. Phys. **114** (5), 836 (2012).

13. A.-K. Jappsen, A. Amann, A. Wacker, E. Scholl, and E. Schomburg, J. Appl. Phys. **92** (6), 3137 (2002).

14. M. Alvaro, M. Carretero, and L. L. Bonilla, EPL **107** (3), 37 002 (2014).

15. V. V. Makarov, G. V. Osipov, V. A. Maksimenko, and A. A. Kharchenko, Tech. Phys. Lett. **41** (1), 69 (2015).

Translated by P. Pozdeev